第 34 卷第 3 期
2018 年 3 月

无 机 化 学 学 报
CHINESE JOURNAL OF INORGANIC CHEMISTRY

Vol.34 No.3
605-613

以三(4-咪唑基苯基)胺为配体的镉配合物的合成、晶体结构和荧光性质

李 健 喻 敏 刘光祥*

(南京晓庄学院环境科学学院,新型功能材料南京市重点实验室,南京 211171)

摘要:以三(4-咪唑基苯基)胺(TIPA)和碘化镉为原料,分别与环已二酸(H_2CDC)和 5-甲基间苯二甲酸(H_2MPDA)在水热条件下反应,得到 2 个结构不同的配位聚合物$[CdI(TIPA)(CDC)_{0.5}]_n$ (**1**)和$\{[Cd(TIPA)(MPDA)]\cdot H_2O\}_n$ (**2**)。对它们进行了元素分析、红外光谱分析,并利用 X 射线衍射测定了它们的单晶结构。单晶结构分析显示,配合物 **1** 拥有二维两重贯穿的(3,4)-连接的$(4.5^2)(4.5^3.7^2)$拓扑结构,层与层之间通过弱相互作用连接成三维超分子结构;而配合物 **2** 具有二维(3,5)-连接的$(4^2.6^7.8)(4^2.6)$拓扑的层状结构,层与层之间通过互锁方式连接成三维金属有机骨架。结果说明了有机羧酸在配合物组装过程中起着非常重要的作用。此外,在室温下对 2 个配合物进行了荧光性质分析。

关键词:镉配合物;三咪唑配体;芳香羧酸配体;晶体结构;荧光性质
中图分类号:O614.24+2 **文献标识码**:A **文章编号**:1001-4861(2018)03-0605-09
DOI:10.11862/CJIC.2018.069

Syntheses, Crystal Structures and Photoluminescent Properties of Two Cadmium(Ⅱ) Coordination Polymers Constructed from Tris(4-imidazolylphenyl)amine

LI Jian YU Min LIU Guang-Xiang*

(*Nanjing Key Laboratory of Advanced Functional Materials, School of Environmental Science, Nanjing Xiaozhuang University, Nanjing* 211171, *China*)

Abstract: Two cadmium(Ⅱ) coordination polymers, $[CdI(TIPA)(CDC)_{0.5}]_n$ (**1**) and $\{[Cd(TIPA)(MPDA)]\cdot H_2O\}_n$ (**2**), (TIPA=tris(4-imidazolylphenyl)amine, H_2CDC=1,4-cyclohexanedicarboxylic acid, H_2MPDA=5-methylisophthalic acid), have been synthesized and characterized by IR spectroscopy, elemental analyses and single-crystal X-ray diffraction. Structural analyses reveal that complex **1** features a rare 2D→2D polyrotaxane network with (3,4)-connected $(4.5^2)(4.5^3.7^2)$ topology, which is further interlinked into a higher-dimensional supramolecular framework by intermolecular weak interactions, whereas complex **2** has a two-dimensional (3,5)-connected novel network with $(4^2.6^7.8)(4^2.6)$ topology and shows a 2D→3D parallel-parallel polycatenation framework. The results show that the carboxylates exert obvious influence on the resulting architectures. Meanwhile, the solid-state photoluminescence of two complexes at room temperature was also investigated. CCDC: 1557335, **1**; 1557336, **2**.

Keywords: cadmium coordination polymer; tris(imidazole) ligands; polycarboxylate; crystal structure; photoluminescence

As an emerging multifunctional solid crystalline materials over the last two decades, metal-organic frameworks (MOFs) have been a hotspot not only for the diversity of architectures and fascinating topol-

收稿日期:2017-10-03。收修改稿日期:2017-11-27。
国家自然科学基金(No.21671107)资助项目。
*通信联系人。E-mail:njuliugx@126.com

ogies but also for potential applications in gas storage and separation, heterogeneous catalysis, fluorescence, chemical sensing, magnetism, electrical energy storage, and so forth[1-7]. Although much progress has been achieved in this field over the past years, it is still a challenge for us to fabricate the desired MOFs with expected structures and properties, because there are varied factors that can affect the structure and property of MOFs[8-12]. From the previously reported studies, it has been demonstrated that organic ligands are crucial in determining the formation of definite MOFs [13-15]. Among various organic ligands, the N-donor ligands as good candidates for the construction of coordination polymers, have aroused a good deal of interests from chemists because of their diversities in coordination modes and conformations[16-17]. It should be noted that, to date, the imidazole-containing N-donor ligands such as 1,4-di(1*H*-imidazol-1-yl)benzene, 4,4′-di(1*H*-imidazol-1-yl)biphenyl, 1,3,5-tri(1*H*-imidazol-1-yl)benzene, 3,3′,5,5′-tetra (1*H*-imidazol-1-yl)biphenyl and 1,3-di(1*H*-imidazol-1-yl)benzene, have been widely used in the construction of various coordination polymers[18-22]. However, the coordination polymers constructed by tri(imidazole) ligands are still in its infancy, although some intriguing examples have been reported[23-27]. Tris(4-imidazolylphenyl)amine (TIPA), as a tridentate bridging ligand, is rarely used in the construction of coordination networks. The TIPA ligand possesses three Ph-imidazole (Ph=phenyl) arms with conformational and geometrical flexibility. The Ph-imidazole arms can rotate freely and adjust itself sterically around the central N moiety when coordinating to the metals[28-32].

In recent years, a number of coordination polymers with various structural types and topological features have been documented[33-35]. In this regard, entangled architectures, including interweaving, polyknotting, polythreading, interdigitation and polycatenation, have been deliberately designed and extensively discussed in several comprehensive reviews[36-37]. Generally, the topological architectures of the coordination polymers can be controlled by the deliberate design and judicious choice of the organic ligands and coordination geometries of the metals[38-39]. In this aspect, the structural features of the organic ligands, such as shape, functionality, flexibility, symmetry, length, and substituent group, can influence structure types of the coordination polymers directly[40-44]. In this work, two coordination p olymers, $[CdI(TIPA)(CDC)_{0.5}]_n$ (**1**) and $\{[Cd(TIPA)(MPDA)]\cdot H_2O\}_n$ (**2**), have been synthesized by using TIPA ligand and different carboxylate anions, where H_2CDC =1,4-cyclohexanedicarboxylic acid and H_2MPDA=5-methylisophthalic acid. The effects of anions on their complex structures are unraveled in detail. Further, the photoluminescent properties of two complexes have also been studied.

1 Experimental

1.1 Materials and general methods

All chemicals and solvents were of reagent grade and used as received without further purification. The TIPA ligand was synthesized according to the reported method[30]. Elemental analyses (C, H and N) were performed on a Vario EL Ⅲ elemental analyzer. Infrared spectra were recorded on KBr discs using a Nicolet Avatar 360 spectrophotometer in the range of 4000 ~400 cm^{-1}. Thermogravimetric analyses (TGA) were performed on a Netzsch STA-409PC instrument in flowing N_2 with a heating rate of 10 ℃·min^{-1}. The luminescent spectra for the powdered solid samples were measured at room temperature on a Horiba FluoroMax-4P-TCSPC fluorescence spectrophotometer with a xenon arc lamp as the light source. In the measurements of emission and excitation spectra the pass width is 5 nm. All the measurements were carried out under the same experimental conditions.

1.2 Synthesis of $[CdI(TIPA)(CDC)_{0.5}]_n$ (1)

A mixture containing CdI_2 (36.6 mg, 0.1 mmol), H_2CDC (17.2 mg, 0.1 mmol), and TIPA (44.3 mg, 0.1 mmol) in DMF/H_2O (1∶1, *V*/*V*) solvent (10 mL) was sealed in a Teflon-lined stainless steel container and heated at 120 ℃ for 3 days. After being cooled down to room temperature, colorless block crystals of **1** were obtained in 57% yield based on TIPA. Anal. Calcd. for $C_{31}H_{25}IN_7O_2Cd$ (%): C, 48.55; H, 3.29; N, 12.79. Found(%): C, 48.47; H, 3.31; N, 12.77. IR (KBr, cm^{-1}): 3 601 (m), 3 089 (w), 1 581 (s), 1 519 (s), 1 364 (s),

1 307 (m), 1087 (m), 1 015 (w), 966 (w), 811 (m), 746 (m), 697 (w), 657 (w), 543 (w).

1.3 Synthesis of {[Cd(TIPA)(MPDA)]·H_2O}$_n$ (2)

Complex **2** was prepared by a process similar to that yielding complex **1** at 120 ℃ by using CdI_2 (36.6 mg, 0.1 mmol), H_2MPDA (17.2 mg, 0.1 mmol), and TIPA (44.3 mg, 0.1 mmol) in DMF/H_2O (1∶1, *V*/*V*) solvent (10 mL). Colorless block crystals of **2** were collected by filtration and washed with water and ethanol several times with a yield of 53% based on TIPA ligand. Anal. Calcd. for $C_{36}H_{29}N_7O_5Cd$ (%): C, 57.49; H, 3.89; N, 13.04. Found (%): C, 57.44; H, 3.91; N, 13.01. IR (KBr, cm^{-1}): 3 416 (m), 3 091 (m), 1 623 (m), 1 553 (m), 1519 (s), 1 431 (m), 1 381 (s), 1 271 (m), 1 032 (m), 913 (m), 828 (w), 734 (s), 654 (m), 542 (w).

1.4 X-ray crystallography

Two block single crystals with dimensions of 0.27 mm×0.25 mm×0.22 mm for **1** and 0.25 mm×0.22 mm×0.19 mm for **2** were mounted on glass fibers for measurement, respectively. X-ray diffraction intensity data were collected on a Bruker APEX Ⅱ CCD diffractometer equipped with a graphite-monochromatic Mo *Kα* radiation (*λ*=0.071 073 nm) using the *φ*-*ω* scan mode at 293(2) K. The diffraction data were integrated by using the SAINT program[45], which was also used for the intensity corrections for the Lorentz and polarization effects. Semi-empirical absorption corrections were applied using the SADABS program[46]. The structures were solved by direct methods using SHELXS-2014[47] and all the non-hydrogen atoms were refined anisotropically on F^2 by the full-matrix least-squares technique with the SHELXL-2014[48] crystallographic software package. The hydrogen atoms, except those of water molecules, were generated geometrically and refined isotropically using the riding model. The pertinent crystallographic data collection and structure refinement parameters are presented in Table 1 and selected bond lengths and angles are listed in Table 2.

CCDC: 1557335, **1**; 1557336, **2**.

Table 1　Crystal data and structure refinement for 1 and 2

Complex	1	2
Formula	$C_{31}H_{25}N_7O_2ICd$	$C_{36}H_{29}N_7O_5Cd$
Formula weight	766.88	752.06
Temperature	293(2)	293(2)
Crystal system	Monoclinic	Monoclinic
Space group	*C*2/*c*	$P2_1/c$
a / nm	2.355 9(2)	1.019 30(9)
b / nm	1.447 25(13)	1.840 95(17)
c / nm	1.866 88(17)	1.885 08(17)
β / (°)	94.745(2)	104.450(2)
V / nm^3	6.343 5(10)	3.425 4(5)
Z	8	4
D_c / ($g·cm^{-3}$)	1.606	1.458
Absorption coefficient / mm	1.701	0.690
θ range / (°)	2.90~25.10	2.86~25.50
F(000)	3 016	1 528
Reflection collected	36 605	50 446
Independent reflection	5 655 (R_{int}=0.050 5)	6 367 (R_{int}=0.051 9)
Reflection observed [$I>2\sigma(I)$]	4 821	5 564
Data, restraint, parameter	5 655, 0, 398	6 367, 55, 480
Goodness-of-fit on F^2	1.043	1.124
R_1, wR_2 [$I>2\sigma(I)$]	0.033 1, 0.082 7	0.058 8, 0.123 1
R_1, wR_2 (all data)	0.041 7, 0.090 0	0.068 7, 0.128 5
$(\Delta\rho)_{max}$, $(\Delta\rho)_{min}$ / ($e·nm^{-3}$)	1 117, −933	1 042, −895

Table 2 Selected bond lengths(nm) and angles(°) for 1 and 2

1					
Cd(1)-O(1)	0.223 0(4)	Cd(1)-N(4)#2	0.236 9(4)	Cd(1)-N(2)	0.229 6(3)
Cd(1)-I(1)	0.279 34(4)	Cd(1)-N(6)#1	0.235 3(3)		
O(1)-Cd(1)-N(2)	139.34(15)	N(6)#1-Cd(1)-N(4)#2	168.09(14)	O(1)-Cd(1)-N(6)#1	88.76(16)
O(1)-Cd(1)-I(1)	106.51(12)	N(2)-Cd(1)-N(6)#1	88.79(13)	N(2)-Cd(1)-I(1)	114.14(9)
O(1)-Cd(1)-N(4)#2	84.19(17)	N(6)#1-Cd(1)-I(1)	94.21(9)	N(2)-Cd(1)-N(4)#2	90.31(14)
N(4)#2-Cd(1)-I(1)	96.99(10)				
2					
Cd(1)-O(1)	0.227 6(4)	Cd(1)-O(4)#5	0.237 4(4)	Cd(1)-N(3)	0.229 4(5)
Cd(1)-N(5)#6	0.238 3(5)	Cd(1)-N(7)#4	0.229 7(5)	Cd(1)-O(3)#5	0.253 1(4)
O(1)-Cd(1)-N(3)	95.18(18)	N(7)#4-Cd(1)-N(5)#6	89.2(2)	O(1)-Cd(1)-N(7)#4	136.02(16)
O(4)#5-Cd(1)-N(5)#6	85.44(19)	N(3)-Cd(1)-N(7)#4	92.35(18)	O(1)-Cd(1)-O(3)#5	136.20(16)
O(1)-Cd(1)-O(4)#5	84.15(15)	N(3)-Cd(1)-O(3)#5	90.98(18)	N(3)-Cd(1)-O(4)#5	89.94(18)
N(7)#4-Cd(1)-O(3)#5	86.76(16)	N(7)#4-Cd(1)-O(4)#5	139.21(16)	O(4)#5-Cd(1)-O(3)#5	52.47(15)
O(1)-Cd(1)-N(5)#6	87.3(2)	N(5)#6-Cd(1)-O(3)#5	83.9(2)	N(3)-Cd(1)-N(5)#6	174.5(2)

Symmetry codes: #1: $-x+1$, $-y+2$, $-z+1$; #2: x, $-y+1$, $z-1/2$ for **1**; #4: $-x+1$, $y+1/2$, $-z+1/2$; #5: $x+1$, y, z; #6: x, $y+1$, z for **2**.

2 Results and discussion

2.1 Crystal structure

Single crystal X-ray diffraction analysis revealed that complex **1** crystallizes in the monoclinic space group *C*2/*c*. The asymmetric unit of complex **1** contains one crystallography independent Cd(Ⅱ) ion, one unique TIPA ligand, one iodide ion and a half CDC^{2-} anion which locates at an inversion center as illustrated in Fig.1. The Cd(Ⅱ) ion is five-coordinated by three nitrogen atoms from three TIPA ligands, one iodide ion and one oxygen atom in a distorted square pyramidal geometry with a τ value of 0.479[49]. The Cd-N bond lengths vary from 0.229 6(3) to 0.236 9(4) nm, and N-Cd-N angles range from 88.79(13)° to 168.09(14)°.

Each TIPA ligand bridges three Cd(Ⅱ) ions to generate a highly undulant 2D sheet with a thickness of *ca.* 1.13 nm (Fig.2). From a topological viewpoint, the sheet can be considered as a 3-connected network with a Schlfli symbol of (4.8^2). There are two kinds of large windows of $Cd_2(TIPA)_2$ and $Cd_4(TIPA)_4$ in the

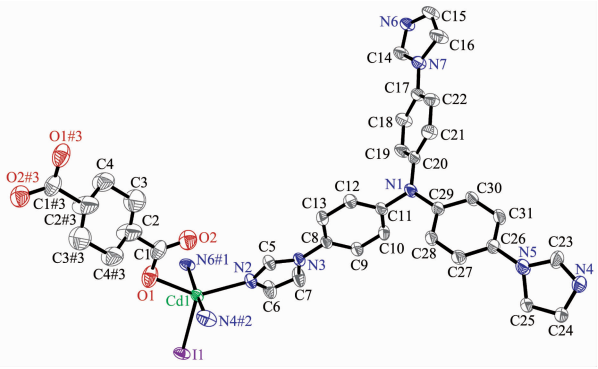

Hydrogen atoms were omitted for clarity; Symmetry codes: #1: $-x+1$, $-y+2$, $-z+1$; #2: x, $-y+1$, $z-1/2$; #3: $-x+1$, $-y+2$, $-z$

Fig.1 Coordination environments of the Cd(Ⅱ) ion in **1** with the ellipsoids drawn at the 30% probability level

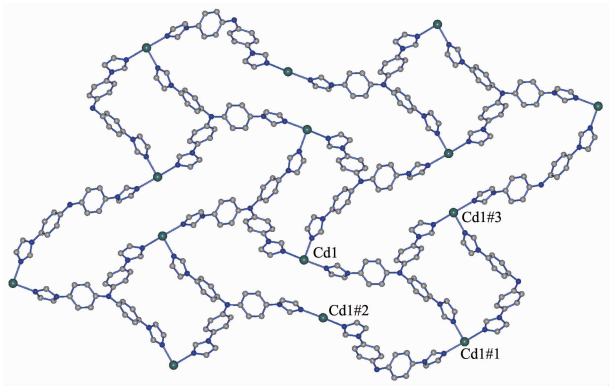

Symmetry codes: #1: x, $-y+1$, $z-1/2$; #2: $1-x$, $2-y$, $-z$; #3: $-x+1$, $y-1$, $1/2-z$

Fig.2 View of a single sheet formed the TIPA ligands and Cd(Ⅱ) ions in **1**

resulting layers. The $Cd_2(TIPA)_2$ window is built up by two Cd(Ⅱ) ions and four Ph-imidazole arms of two different TIPA ligands with the dimension of 1.202 nm×1.529 nm, while the $Cd_4(TIPA)_4$ unit is built up by four Cd(Ⅱ) ions and eight Ph-imidazole arms of four ligands with the dimension of 1.126 nm×3.335 nm. It is noteworthy that each $Cd_4(TIPA)_4$ unit is divided into two $Cd_2(TIPA)_2(CDC)$ subunit by CDC anion linking two Cd(Ⅱ) ions to give an undulate 2D layer. Topologically, the TIPA ligand can be considered as a 3-connected node, the CDC anions can be considered as linkers, and Cd(Ⅱ) ions can be regarded as 4-connected nodes. Therefore, the 2D layer of **1** is a (3,4)-connected topology with Schläfli symbol of $(4.5^2)(4.5^3.7^2)$ (Fig.3).

The most fascinating structural feature of **1** is that two such layers are interlaced each other in a parallel fashion to give a 2D →2D polyrotaxane network (Fig.4). The Cd_2TIPA_2 windows of each layer are passed by CDC anions of adjacent layer, and each $Cd_2(TIPA)_2(CDC)$ unit of each layer is threaded through by one armed rod of the TIPA ligand from adjacent layers. More interestingly, the neighboring 2D polyrotaxane sheets are parallel with each other.

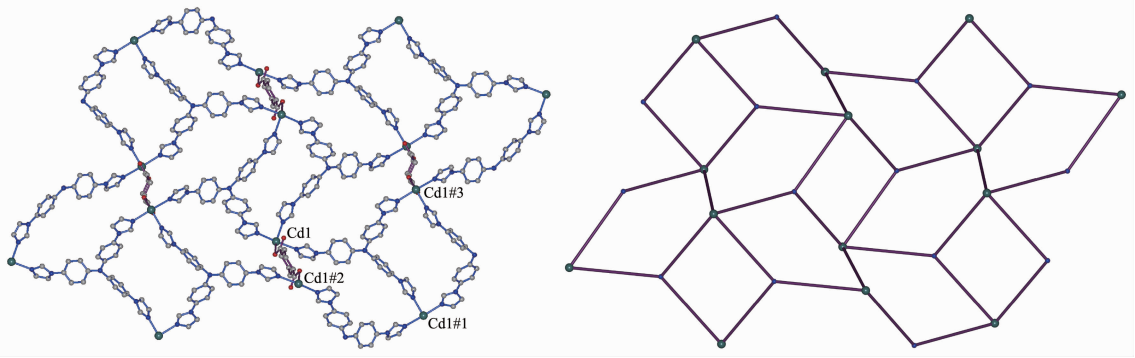

Symmetry codes: #1: x, $-y+1$, $z-1/2$; #2: $1-x$, $2-y$, $-z$; #3: $-x+1$, $y-1$, $1/2-z$

Fig.3　Undulate layer and schematic representation of the (3,4)-connected framework with $(4.5^2)(4.5^3.7^2)$ topology of **1**

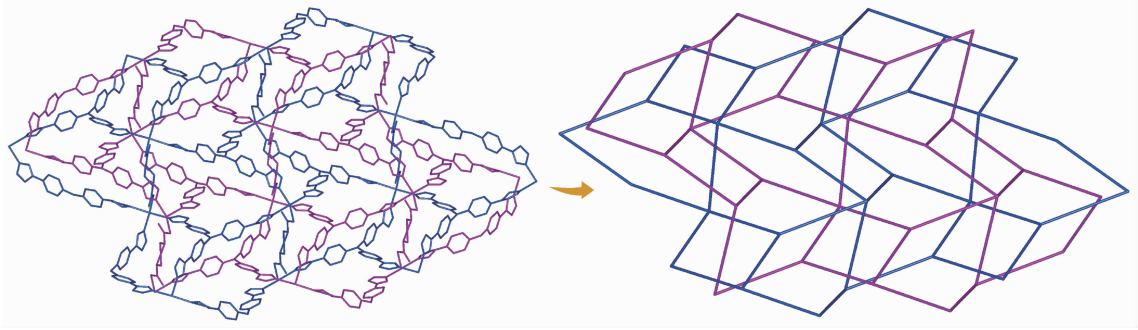

Fig.4　2D→2D polyrotaxane network in **1**

When the ligand H_2MPDA was used instead of H_2CDC to react with Cd(Ⅱ) salts under hydrothermal conditions, complex **2** was isolated. Complex **2** crystallizes in the monoclinic space group $P2_1/c$. The asymmetric unit consists of one Cd(Ⅱ) ion, one TIPA ligand, and one lattice water molecule. The local coordination geometry around the Cd(Ⅱ) ion is depicted in Fig.5. The Cd(Ⅱ) ion adopts a distorted octahedral coordination sphere that is defined by three oxygen atoms from two distinct $MPDA^{2-}$ anions and three nitrogen atoms from three different TIPA ligands; thus, the Cd(Ⅱ) ions can be considered as 5-connecting nodes. Each TIPA links three Cd(Ⅱ) ions, acting as a 3-connecting node to form a 1D ladder-like chain. Two carboxylate groups of the $MPDA^{2-}$ anions adopting monodentate and bidentate chelate coordination modes bridge two Cd(Ⅱ) ions, and $MPDA^{2-}$ joins adjacent parallel chains as a pillar connector to form a 2D grid like (4,4) bilayer (Fig.6). The Schläfli symbol for this binodal net is $(4^2\cdot6^7\cdot8)(4^2\cdot6)$. Viewed from the b axis, there exist

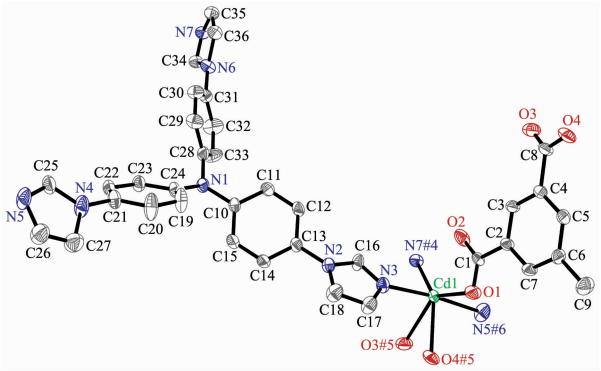

Hydrogen atoms and lattice water molecules were omitted for clarity; Symmetry codes: #4: $-x+1$, $y+1/2$, $-z+1/2$; #5: $x+1$, y, z; #6: x, $y+1$, z

Fig.5 Coordination environments of the Cd(Ⅱ) ion in **2** with the ellipsoids drawn at the 30% probability level

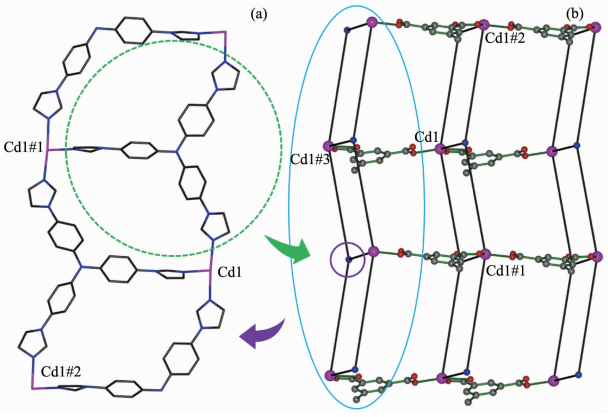

TIPA ligand is simplified to a 3-connecting node for clarity; Symmetry codes: #1: $1-x$, $1/2+y$, $1/2-z$; #2: $1-x$, $y-1/2$, $1/2-z$; #3: $-1+x$, y, z

Fig.6 View of the ladder-like chain (a) and perspective view of the 2D grid-like (4,4) bilayer (b) in **2**

rectangular channels with a cross section of approximately 2.04 nm×1.09 nm (excluding van der Waals radii). The channel is so large that the two other equivalent bilayers can be accommodated in that channel. This may be the mainly reason to form the 2D→3D parallel entangled structure. Upon interpenetration, complex **2** just contains a small solvent accessible void space of 2.8% of the total crystal volume, according to a calculation performed using PLATON[50].

The topological feature of complex **2** is most unusual because it is a rarely observed bilayer motif which is parallel-parallel catenated with two other equivalent adjacent ones to form a 3D supramolecular structure (Fig.7). To our knowledge, this (3,5)-connected bilayer is yet to be reported. Compared to 2D→3D polycatenation systems in parallel-parallel inclined fashion or parallel-parallel highly undulating fashion, fewer examples of 2D→3D parallel entangled structures have been observed[51-52].

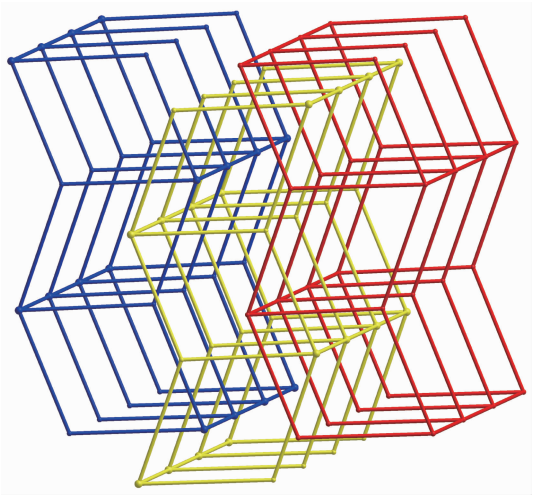

Fig.7 Perspective view of the 2D→3D parallel entangled structures in **2**

2.2 FT-IR spectra

The IR spectra of **1** and **2** show the absence of the characteristic bands at around 1 700 cm^{-1} attributed to the protonated carboxylate group, which indicates that the complete deprotonation of H_2CDC and H_2MPDA ligands upon reaction with Cd(Ⅱ) ion. The presence of vibrational bands of 1 650~1 550 cm^{-1} are characteristic of the asymmetric stretching of the deprotonated carboxylic groups of CDC^{2-} and $MPDA^{2-}$ anions. The difference between asymmetric and symmetric carbonyl stretching frequencies ($\Delta\nu=\nu_{asym}-\nu_{sym}$) was used to fetch information on the metal-carboxylate binding modes. Complex **1** showed a pairs of ν_{asym} and ν_{sym} frequencies at 1 584, 1 354 cm^{-1} corresponding to the carbonyl functionality of dicarboxylate ligand indicating a symmetric monodentate coordination mode ($\Delta\nu$=230 cm^{-1}). Complex **2** shows two pairs of ν_{asym} and ν_{sym} frequencies at 1 623, 1 431 cm^{-1} ($\Delta\nu$=192 cm^{-1}) and 1 553, 1 381 cm^{-1} ($\Delta\nu$=172 cm^{-1}) for the carbonyl functionality indicating two coordination modes as observed in the crystal

structure. OH stretching broad bands at 3 416 cm^{-1} for **2** are attributable to the lattice water. The bands in the region of 640~1 250 cm^{-1} are attributed to the -CH- in-plane or out-of-plane bend, ring breathing, and ring deformation absorptions of benzene ring, respectively. The IR spectra exhibit the characteristic peaks of imidazole groups at *ca.* 1 520 cm^{-1} [53].

2.3 Thermal stability

The thermal behaviors of complexes **1** and **2** were measured under a dry N_2 atmosphere at a heating rate of 10 ℃·min^{-1} from 25 to 800 ℃ and the TG curves are presented in Fig.8. The TGA curve of **1** reveals that no obvious weight loss is observed until the temperature reaches 340 ℃. The anhydrous compound decomposes from 340 to 800 ℃, indicating the release of organic components. For **2**, the first weight loss of 2.61% (Calcd. 2.39%) occurs in the range of 60~150 ℃, indicating the loss of one free water molecules. Then, the framework of **2** decomposes gradually above 270 ℃.

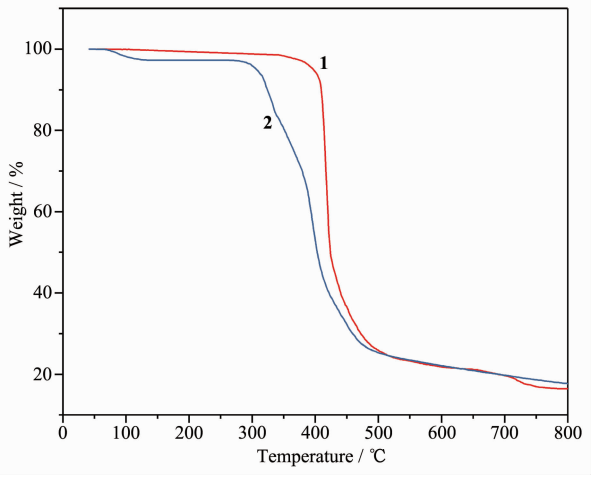

Fig.8　TGA curves of complexes **1** and **2**

2.4 Photoluminescent properties

Photoluminescence properties of Cd(Ⅱ) complexes have attracted intense interest due to their potential applications in photochemistry, chemical sensors, and electroluminescent display[54-55]. The photoluminescent properties of **1**, **2** and TIPA ligand were investigated in solid state at room temperature (Fig.9). The TIPA ligand exhibits emission band with a maximum at 422 nm upon excitation at 365 nm, which may be assigned to $\pi^*\rightarrow n$ or $\pi^*\rightarrow\pi$ transitions of the ligands[56-57].

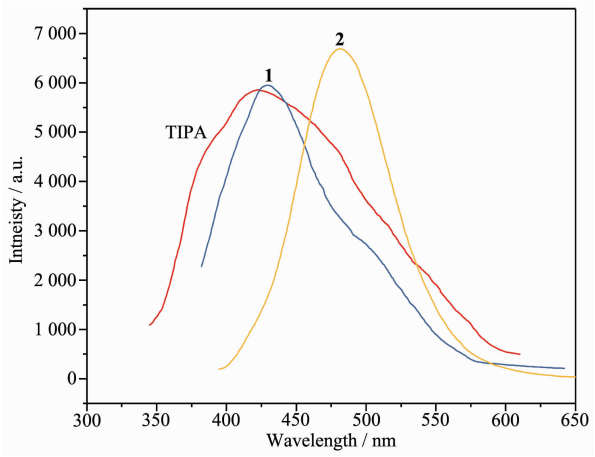

Fig.9　Solid-state photoluminescent spectra of complexes **1~2** and TIPA ligand

The emission peaks of complexes occur at 429 nm (λ_{ex}=370 nm) for **1**, 482 nm (λ_{ex}=380 nm) for **2**. Under the same experimental conditions, the emission intensities of free H_2CDC and H_2MPDA are weaker than that of TIPA ligand, so it is considered that it has no significant contribution to the fluorescent emission of the complexes with the presence of TIPA ligand. The emission of **1** can be essentially ascribed to the intraligand fluorescent emission. The red-shift of the emission can be attributed to the ligand coordination to the metal center, which effectively increases the rigidity of the ligand and reduces the loss of energy by radiationless decay. However, the intense blue emission peak at 481 nm (λ_{ex}=380 nm) for **2** is highly red-shifted with respect to the free TIPA ligands. The intense fluorescence of **2** indicates that a strong interaction exists between the ligand and the Cd(Ⅱ) ion[58-60].

References:

[1] Gamage N D H, McDonald K A, Matzger A J. *Angew. Chem., Int. Ed.*, **2016**,**55**:12099-12103

[2] Noh T H, Jung O S. *Acc. Chem. Res.*, **2016**,**49**:1835-1843

[3] Maza W A, Padilla R, Morris A J. *J. Am. Chem. Soc.*, **2015**, **137**:8161-8168

[4] Manna P, Das S K. *Cryst. Growth Des.*, **2015**,**15**:1407-1421

[5] He H M, Song Y, Sun F X, et al. *Cryst. Growth Des.*, **2015**, **15**:2033-2038

[6] Li S L, Xu Q. *Energy Environ. Sci.*, **2013**,**6**:1656-1683

[7] Zheng J, Wu M Y, Jiang F L, et al. *Chem. Sci.*, **2015**,**6**:3466-3470

[8] Long L S. *CrystEngComm*, **2010**,**12**:1354-1365

[9] Tan Y X, He Y P, Zhang Y, et al. *CrystEngComm*, **2013**,**15**:6009-6014

[10]Huang S Y, Li J Y, Li J Q, et al. *Dalton Trans.*, **2014**,**43**:5260-5264

[11]Zhang J W, Kan X M, Liu B Q, et al. *Chem. Eur. J.*, **2015**,**21**:16219-16228

[12]Zhao X L, Sun W Y. *CrystEngComm*, **2014**,**16**:3247-3258

[13]WU Qi(吴琪), SU Zhi(苏志), WANG Hong-Yan(王红艳), et al. *Chinese J. Inorg. Chem.*(无机化学学报), **2017**,**33**(10):1889-1895

[14]Han L J, Yan W, Chen S G, et al. *Inorg. Chem.*, **2017**,**56**:2936-2940

[15]He Y F, Chen D M, Xu H, et al. *CrystEngComm*, **2015**,**17**:2471-2478

[16]Huang Y Q, Chen H Y, Li Z G, et al. *Inorg. Chim. Acta*, **2017**,**466**:71-77

[17]Dong X Y, Si C D, Fan Y, et al. *Cryst. Growth Des.*, **2016**,**16**:2062-2073

[18]Ke C H, Lin G R, Kuo B C, et al. *Cryst. Growth Des.*, **2012**,**12**:3758-3765

[19]Wang F, Ke X H, Zhao J B, et al. *Dalton Trans.*, **2011**,**40**:11856-11865

[20]Su Z, Fan J, Okamura T A, et al. *Cryst. Growth Des.*, **2010**,**10**:1911-1922

[21]Luo L, Wang P, Xu G C, et al. *Cryst. Growth Des.*, **2012**,**12**:2634-2645

[22]Schlechte L, Bon V, Grunker R, et al. *Polyhedron*, **2012**,**44**:179-186

[23]Su Z, Xu J, Fan J, et al. *Cryst. Growth Des.*, **2009**,**9**:2801-2811

[24]Fan J, Sun W Y, Okamura T A, et al. *Inorg. Chem.*, **2003**,**42**:3168-3175

[25]Fan J, Gan L, Kawaguchi H, et al. *Chem. Eur. J.*, **2003**,**9**:3965-3973

[26]Liu H K, Sun W Y, Ma D J, et al. *Chem. Commun.*, **2000**:591-592

[27]Liu F H, Chen W Z, You X Z. *J. Solid State Chem.*, **2002**,**169**:199-207

[28]Wu H, Liu H Y, Liu Y Y, et al. *Chem. Commun.*, **2011**,**47**:1818-1820

[29]Yao X Q, Cao D P, Hu J S, et al. *Cryst. Growth Des.*, **2011**,**11**:231-239

[30]Wu H, Liu H Y, Liu B, et al. *CrystEngComm*, **2011**,**13**:3402-3407

[31]Wu H, Liu H Y, Yang J, et al. *Cryst. Growth Des.*, **2011**,**11**:2317-2324

[32]Wu H, Liu B, Yang J, et al. *CrystEngComm*, **2011**,**13**:3661-3664

[33]Alezi D, Spanopoulos I, Tsangarakis C, et al. *J. Am. Chem. Soc.*, **2016**,**138**:12767-12770

[34]Gu J Z, Liang X X, Cai Y, et al. *Dalton Trans.*, **2017**,**46**:10908-10925

[35]Duan J G, Higuchi M, Kitagawa S. *Inorg. Chem.*, **2015**,**54**:1645-1649

[36]Batten S R. *CrystEngComm*, **2001**,**3**:67-72

[37]Carlucci L, Ciani G, Proserpio D M. *Coord. Chem. Rev.*, **2003**,**246**:247-289

[38]Dinca M, Yu A F, Long J R. *J. Am. Chem. Soc.*, **2006**,**128**:8904-8913

[39]Zhang L P, Ma J F, Yang J, et al. *Inorg. Chem.*, **2010**,**49**:1535-1550

[40]Reger D L, Wright T D, Semeniuc R F, et al. *Inorg. Chem.*, **2001**,**40**:6212-6219

[41]Zaman M B, Smith M D, zur Loye H C. *Chem. Commun.*, **2001**:2256-2257

[42]Kitaura R, Seki K, Akiyama G, et al. *Angew. Chem., Int. Ed.*, **2003**,**42**:428-431

[43]Kitaura R, Fujimoto K, Noro S, et al. *Angew. Chem., Int. Ed.*, **2002**,**41**:133-135

[44]Qi Y, Luo F, Che Y X, et al. *Cryst. Growth Des.*, **2008**,**8**:606-611

[45]*SMART* and *SAINT*, *Program for Data Extraction and Reduction*, Bruker AXS, Inc., Madison, Wisconsin, USA, **2002**.

[46]Sheldrick G M. *SADABS, Program for Empirical Absorption Correction of Area Detector Data*, University of Göttingen, Germany, **2003**.

[47]Sheldrick G M. *SHELXS*-2014, *Program for Crystal Structure Solution*, University of Göttingen, Germany, **2014**.

[48]Sheldrick G M. *SHELXL*-2014, *Program for the Refinement of Crystal Structure*, University of Göttingen, Germany, **2014**.

[49]Addison A W, Rao T N. *J. Chem. Soc. Dalton Trans.*, **1984**:1349-1356

[50]Spek A L. *J. Appl. Crystallogr.*, **2003**,**36**:7-13

[51]Zhang J, Chew E, Chen S, et al. *Inorg. Chem.*, **2008**,**47**:3495-3497

[52]Wu H, Ma J F, Liu Y Y, et al. *CrystEngComm*, **2011**,**13**:7121-7128

[53]Nakamoto K. *Infrared and Raman Spectra of Inorganic and Coordinated Compounds*. *5th Ed*. New York: John Wiley & Sons, **1997**.

[54]Thirumurugan A, Natarajan S. *Dalton Trans*., **2004**:2923-2928

[55]McGarrah J E, Kim Y J, Hissler M, et al. *Inorg. Chem.*, **2001**,**40**:4510-4511

[56]Wen L L, Lu Z D, Lin J G, et al. *Cryst. Growth Des*., **2007**, **7**:93-99

[57]Lin J G, Zang S Q, Tian Z F, et al. *CrystEngComm*, **2007**,**9**: 915-921

[58]Liu H J, Tao X T, Yang J X, et al. *Cryst. Growth Des*., **2008**,**8**:259-264

[59]Klessinger J M, Michl J. *Excited States and Photochemistry of Organic Molecules*. New York: VCH, **1995**.

[60]XU Han(徐涵). *Chinese J. Inorg. Chem.*(无机化学学报), **2016**,**32**(8):1481-1486